ACS OMEGA

Open Access

http://pubs.acs.org/journal/acsodf

Article

CO_2/H_2 Separation by Synergistic Enhanced Hydrate Method with SDS and R134a

Tian Qi, Mengfei Liu, Zihan Lu, Qianhao Zhang, Miao Yang, Lanlan Jiang, Yanqiu Xiao,* Wenfeng Hu, Runfeng Tian, and Chuanxiao Cheng*

Cite This: *ACS Omega* 2024, 9, 30234−30243

Read Online

ACCESS | Metrics & More | Article Recommendations

ABSTRACT: The synergistic effect of thermodynamic promoter tetrafluoroethane (R134a) and kinetic promoter sodium dodecyl sulfate (SDS) can significantly improve the phase equilibrium conditions required for CO_2 hydrate formation and promote rapid generation of CO_2 hydrate. Based on this, this study investigates the influence of SDS and R134a synergy on the separation of CO_2/H_2 mixed gas using the hydrate method. The research reveals that without SDS addition, R134a hydrate forms first at the gas−liquid interface before CO_2 hydrate induction, hindering gas−liquid exchange. The addition of SDS can inhibit the formation of the hydrate film, enhance the initiator effect of R134a in the CO_2 hydrate formation process, accelerate the nucleation of CO_2 hydrate, and thus synergistically strengthen the separation of CO_2/H_2 mixed gases. Hydrate formation can be achieved at a concentration of 100 ppm of SDS solution, and the synergistic growth effect of R134a and CO_2 hydrate becomes more significant with increasing SDS concentration. Optimal separation efficiency and maximum H_2 concentration are achieved at 500 ppm of SDS, with 42.29 and 54.88% separation efficiency and H_2 concentration, respectively. Decreasing the initial charge temperature has little impact on separation efficiency but significantly reduces the induction time, reducing it to 3 min at 12 °C. This study improved the separation efficiency of CO_2 and H_2 mixed gas, providing a better reference for hydrogen purification by the hydrate method.

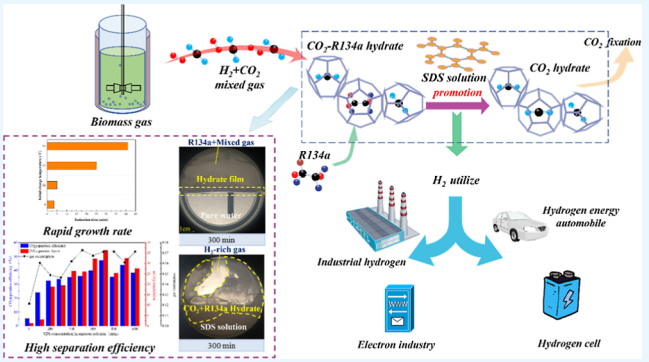

1. INTRODUCTION

The rapidly growing demand for renewable energy has led many countries to seek alternatives for fossil fuels.[1,2] Hydrogen, a clean and green energy source, possesses broad applications in power generation, chemical, and petrochemical industries.[3,4] H_2-CO_2 mixed gases are extensively present in industrial and biomass blends. However, the low H_2 content renders it unusable, necessitating reliable and economical methods for separating CO_2 and purifying H_2. Compared to traditional absorption, adsorption, and low-temperature distillation methods,[5−8] hydrate-based gas separation technologies (HBGS) offer advantages such as easy availability of raw materials, high separation efficiency, and mild reaction conditions.[9] Present research on HBGS primarily focuses on fuel gases, biogas, shale gas, and flue gas.[10] By forming CO_2 hydrates, gases containing CO_2 are fixed in the solid phase, with CO_2 compositions ranging from 30 to 60% in the research. Consequently, HBGS is also applicable to capturing CO_2 generated during biomass hydrogen production (40−60%)[11] to obtain pure hydrogen energy. Economic cost calculations for specific cases of this method demonstrate that it is more economically viable than traditional separation techniques.[12,13]

The fundamental principle of separating CO_2/H_2 mixed gases using the gas hydrate method is based on the distinct phase equilibrium conditions required for hydrogen and carbon dioxide to form hydrates. By controlling the temperature and pressure during the gas hydrate formation process, carbon dioxide is first converted into a solid hydrate, resulting in an increased concentration of hydrogen in the gas phase. Following the gas−solid separation, the CO_2 hydrate can be decomposed through temperature elevation or pressure reduction, releasing the CO_2 gas component enriched in the hydrate phase and achieving the separation of H_2/CO_2 mixed gases (Figure 1). Due to the significantly lower phase equilibrium pressure required for CO_2 to form hydrates compared to H_2,[14,15] the hydrate captures a higher amount of CO_2. However, there are existing challenges in the research of hydrate-based CO_2 separation, such as the low

Received: January 5, 2024
Revised: May 16, 2024
Accepted: May 21, 2024
Published: July 5, 2024

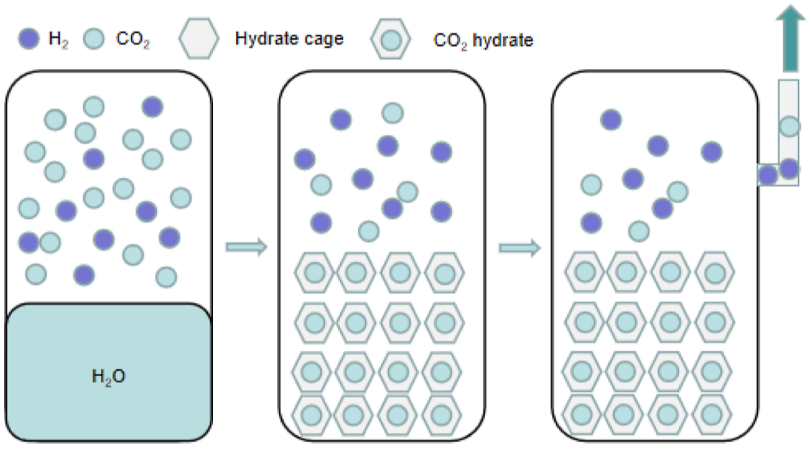

Figure 1. Principle of hydrate-based separation of the CO_2/H_2 gas mixture.

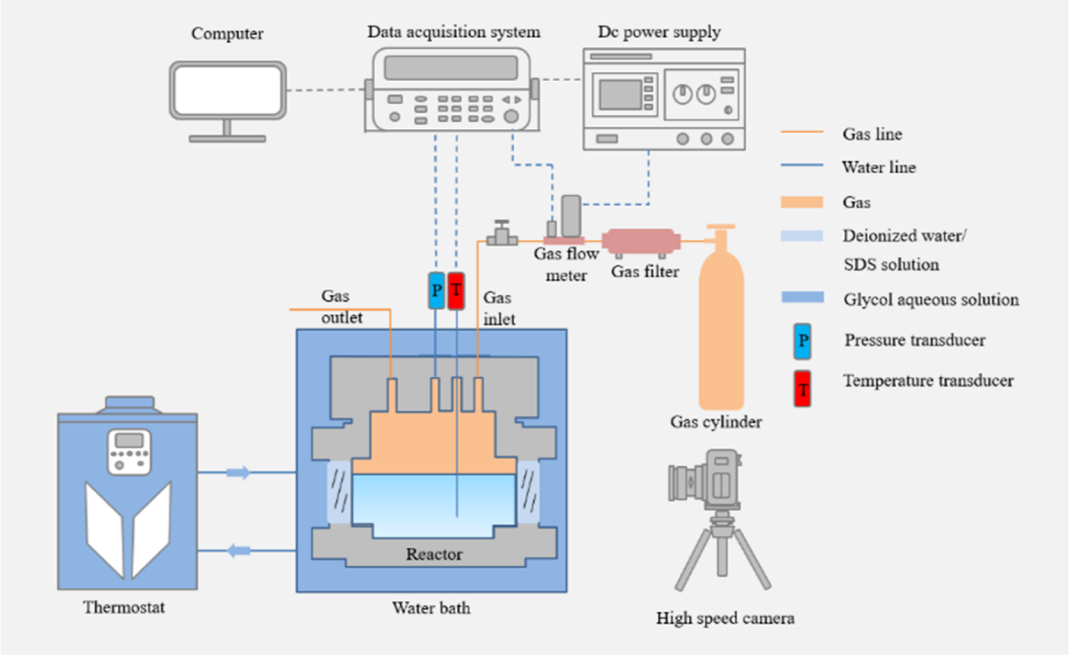

Figure 2. Diagram of the experimental setup.

rate of hydrate formation and inadequate separation efficiency caused by low CO_2 partial pressure. These defects can be overcome by employing suitable additives.

Chemical additives can be broadly categorized into thermodynamic promoters and kinetic promoters.[16] Thermodynamic promoters involve direct participation in the formation of hydrate crystal structures, thereby alleviating the required temperature/pressure conditions for hydrate generation. Some commonly used thermodynamic promoters include tetrahydrofuran (THF), tetrabutylammonium bromide (TBAB), and cyclopentane (CP). As an outstanding thermodynamically water-soluble additive, THF is currently widely employed in hydrate-based separation research. Babu et al.[17] found that THF can effectively promote the generation of CO_2 hydrate, but due to the volatile nature of THF, the gas phase is often mixed with THF during the separation process, and it is necessary to separate the THF in the residual gas phase, which increases the separation cost. Due to its volatility, the gaseous phase often contains THF during the separation process, necessitating the removal of residual THF, thereby increasing separation costs. As for TBAB,[18] it was found that the half-cage structure of TBAB hydrate encapsulates some H_2 into the hydrate, which affects the separation of the mixture. The high prices of THF and TBAB restrict their large-scale application. Due to the insolubility of CP in water, its use in industrial applications can lead to severe layering phenomena, increased gas−liquid mass transfer resistance, decreased dissolved gas levels in water during hydrate formation, and thus compromised CO_2 separation efficiency using the hydrate method.[16]

The search for clean and efficient additives in the hydrate-based separation of CO_2/H_2 mixtures holds significant importance. 1,1,1,2-tetrafluoroethane (R134a) has zero ozone depletion potential and a global warming potential of 1430, and its large-scale use as a refrigerant will be globally banned. However, as a thermodynamic promoter for trace use of hydrates, it exhibits favorable characteristics due to its mild phase equilibrium conditions, excellent chemical stability, and exclusive involvement in physical reactions during hydrate formation. Furthermore, owing to its low boiling point, R134a facilitates easy separation. It demonstrates commendable

https://doi.org/10.1021/acsomega.3c09839
ACS Omega 2024, 9, 30234−30243

properties in promoting the rapid generation of CO_2 hydrates. Studies indicate that R134a actively participates in the formation of both pure R134a hydrates and R134a/CO_2 mixed hydrates, both adopting a type II structure.[19] Additionally, investigations by Song et al.[20] reveal that the inclusion of R134a significantly reduces the induction time for pure CO_2 hydrate formation. The kinetic promoter dodecyl sodium sulfate (SDS) enhances the gas exchange rate at the gas−liquid interface, thereby augmenting the rate of CO_2 hydrate formation and gas consumption.[21] In summary, the synergistic utilization of R134a and SDS holds great potential in promoting CO_2 hydrate formation, presenting an avenue for further exploration of the mechanisms underlying the enhancement of CO_2/H_2 mixture separation.

This project proposes a synergistic enhancement approach using SDS and R134a for the hydrate-based separation of CO_2/H_2 mixed gases. By synergistically employing the thermodynamic promoter R134a and the kinetic promoter SDS to reinforce CO_2 hydrate formation, the separation of CO_2/H_2 mixed gases is facilitated. The study systematically investigates the influence of SDS concentration and initial charge temperature on the nucleation and growth processes of CO_2 hydrates. Furthermore, it quantitatively analyzes the collaborative effects of the two promoters on the separation efficiency of H_2, elucidating the intrinsic relationship between promoters and hydrate formation. A new theoretical method is provided for the separation of CO_2/H_2 gas mixtures based on hydrates.

2. EXPERIMENTAL MATERIALS AND METHODS

Figure 2 demonstrates a self-built experimental system designed for visualizing the generation of CO_2/H_2 mixed hydrates, consisting of a high-pressure reactor, a constant temperature bath, an image acquisition system, a temperature and pressure sensor, and a data acquisition system. The reactor, with a volume of 800 mL, is fabricated from 316 stainless steel and features two quartz windows on both sides, capable of withstanding up to 10 MPa of pressure. A cooling ethylene glycol external circulation device (XT5718RC-E800L, Hangzhou Xue Zhong tan Technology Co., Ltd.) is employed for temperature regulation inside the reactor and provision of a low-temperature environment. The temperature sensor (PT-1000JM608I, Hefei Zhongding Information Technology Co., Ltd.) offers a measurement range of −15 to 200 °C (±0.2%). The pressure sensor (UNIK 5000, PTX5072-TB-A1-CA-H0-PA, General Electric Detection Control Technology Co., Ltd.) covers a range of 0−25 MPa with an accuracy of 0.25% FS. The image acquisition system (EOS 6D) captures visual data of hydrate transformations at intervals of 30 s. Data from the experiment are recorded by a data acquisition instrument and computer, supplemented by a gas chromatography instrument (A60, Changzhou Xinnuo Instrument Co., Ltd.). Experimental materials include CO_2/H_2, with a mixed gas molar ratio of 60:40 (Henan Yuanzheng Technology Development Co., Ltd.), 1,1,1,2-tetrafluoroethane (CH_2FCF_3, R134A, Shandong Dongyue Chemical Co., Ltd.), and sodium dodecyl sulfate (SDS, Tianjin Fengzhou Chemical Reagent Technology Co., Ltd.). These gases are transferred between supply containers and reactors, and then back to the supply containers several times. All aqueous solutions are prepared using deionized water (with a resistance of 16−18 MΩ cm).

The experiment uses a partial pressure blending method to prepare R134a/CO_2/H_2 mixed gas, with R134a and CO_2/H_2 mixed gas entering the supply container sequentially. This process is controlled by gas flow meters and pressure curves. These gases are then transferred from the supply vessel to the reactor using a booster pump and from the reactor to the supply vessel several times. All gas mixing processes are conducted at a constant temperature to obtain the accurate composition, while ensuring a CO_2 partial pressure of 2.6 MPa. The volume of gas initial charge into the supply container is calculated using the Peng−Robinson state equation[22] and verified by the gas flow meter. The SDS solution is prepared by mixing the appropriate amounts of SDS and deionized water, stirring at 400 rpm at 30 °C for 30 min to obtain the required SDS solution for the experiment.

- Initially, experiments were conducted to investigate the formation of hydrates from a CO_2/H_2 mixture under 3.5_{mol} % R134a conditions.
- Subsequently, experiments were performed to examine hydrate formation with R134a in the presence of SDS aqueous solutions of varying concentrations.
- Finally, hydrate growth experiments were carried out at different gas charging temperatures. The data acquisition system recorded the time of hydrate formation, as well as changes in temperature and pressure, allowing for the calculation of gas consumption throughout the entire experimental process.

Based on the experimental conditions, the initial temperature T_0 was set, with a CO_2 partial pressure of 2.6 MPa and a total pressure of 4.4 MPa to ensure consistent CO_2 content during the experiment. The induction time is judged by the exothermic peaks on the pressure reduction curve and temperature cooling curve in the reactor based on the start time of the reactor starting to cool down as the start time. Prior to the experiment, the reaction vessel was cleaned with deionized water and then filled with 400 g of deionized water or 400 g of SDS solution, after which it was placed in ethylene glycol solution. The reaction vessel was purged 3 times with a prepared R134a/CO_2/H_2 mixed gas to remove the air inside the vessel, and the water bath temperature was set to 9 °C before slowly pressurizing to the experimental pressure. Then, the water bath temperature was set to the experimental temperature of 2 °C. At 300 min of reaction, the pressure and temperature in the reaction vessel remained basically unchanged, indicating that the hydrate deposition sample was generated completely and the experiment was ended. During the reaction process, the changes in hydrate occurrence were recorded by a camera, and all experimental temperature and pressure data were automatically recorded every 30 s by a data logger. After the experiment, gas sampling was carried out using 100 mL sampling bags, resulting in a total of approximately 100 mL (0.0055 mol) of gas being sampled, which was basically negligible compared to the initial gas volume.

Based on the temperature and pressure values of the gas phase in the reaction vessel, the amount of gas consumed during the experimental process can be calculated using the gas state equation.

$$\Delta n = \left(\frac{pV}{ZRT}\right)_0 - \left(\frac{pV}{ZRT}\right)_t \quad (1)$$

The gas occupies a volume of 400 cm^3, P represents the pressure of the gas phase, T represents the temperature of the gas phase, and R is the gas constant, where $R = 8.314 J\cdot(mol\cdot K)^{-1}$. The compressibility factor Z can be determined using Pitzer's equation.,[17,23−26] the amount of gas consumed during the

https://doi.org/10.1021/acsomega.3c09839
ACS Omega 2024, 9, 30234−30243

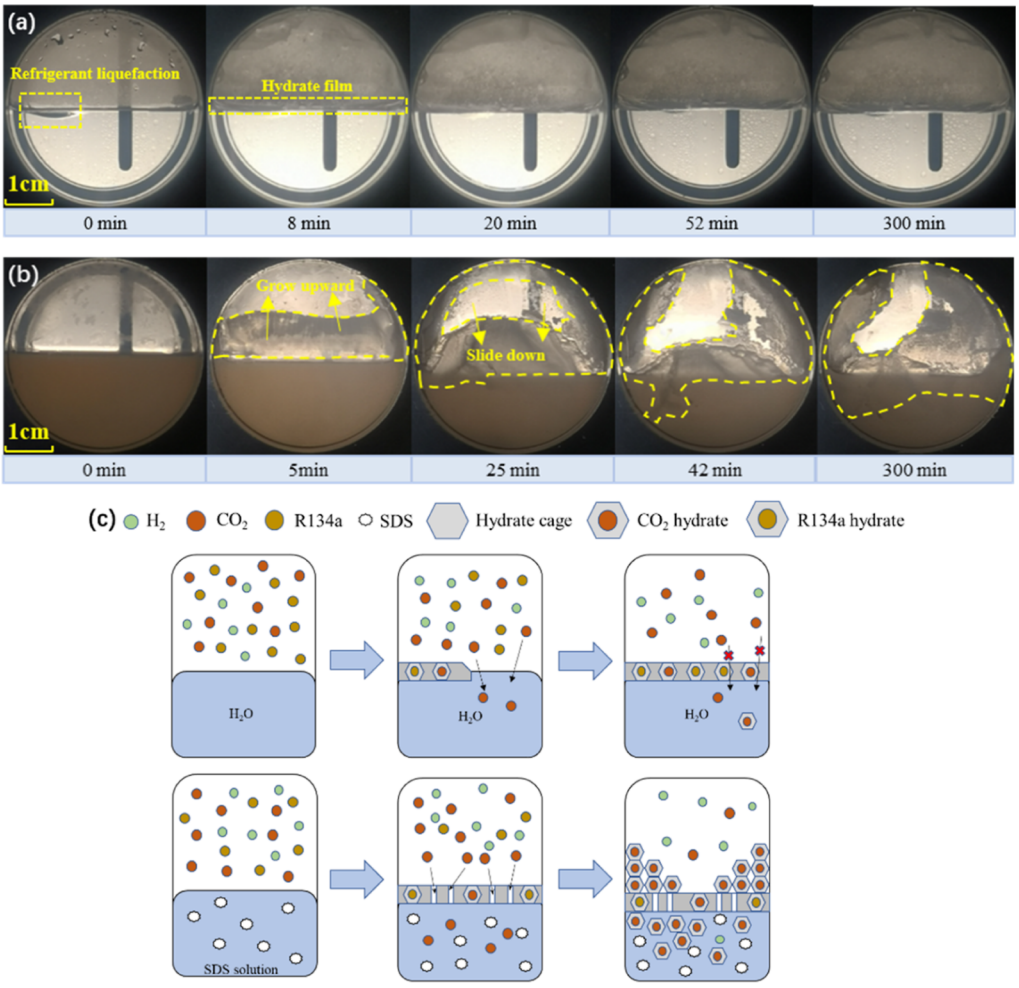

Figure 3. Growth behavior of hydrates in a 3.5_{mol} % R134a coupled with (a) 0 ppm and (b) 500 ppm of SDS aqueous solutions. (c) Schematic diagram of the growth mechanism evolution under the synergistic promotion effect of R134a and SDS.

experimental process can be calculated (including dissolved and consumed in the hydrate).

$$Z = 1 + B^0\frac{p_r}{T_r} + \omega B^1\frac{p_r}{T_r} \tag{2}$$

In order to evaluate the effectiveness of the hydrate method for the purification of H_2, the separation efficiency of CO_2 gas was calculated by eq 3.[27] $n_{CO_2}^{C}$, $n_{CO_2}^{feed}$, respectively, expressed as the molar amount of CO_2 consumed in the hydrate formation (mol); molar amount of CO_2 in feedstock gas (mol).

$$\text{S. Fr.} = \frac{n_{CO_2}^{C}}{n_{CO_2}^{feed}} \times 100\% \tag{3}$$

The separation factor S.F. of CO_2 was calculated by eq 4.[27]

$$\text{S. F.} = \frac{n_{CO_2}^{C} \times n_{H_2}^{RG}}{n_{CO_2}^{RG} \times n_{H_2}^{C}} \tag{4}$$

$n_{CO_2}^{C}$, $n_{H_2}^{C}$, $n_{H_2}^{RG}$, and $n_{CO_2}^{RG}$, respectively, expressed as the amount of CO_2 and H_2 consumed in the hydrate formation (mol), the amount of CO_2 and H_2 in the residual gas phase at the end of the hydrate formation (mol), respectively. S.F. is separation factor. When S.F. > 1, the method has a CO_2 separating effect and the larger the value of S.F., the better the separating effect is.[27]

In order to measure the consumption of the gas mixture, t_{end} is defined as the effective response time, which is the duration from the beginning until the pressure change inside the reactor is less than 0.1 MPa/min ($\Delta P < 0.1$ MPa·min^{-1}). The average pressure drop rate ΔP_m was used to reflect the gas consumption rate.

$$\Delta P_m = \frac{\Delta P}{t_{end}} \tag{5}$$

3. RESULTS AND DISCUSSION

3.1. Growth Characteristics of CO_2/H_2 Gas Mixture Hydrate Enhanced by SDS Synergized with R134a. In the absence of SDS, the process of 3.5_{mol} % R134a/CO_2/H_2 hydrate formation is depicted in Figure 3a. After completing the charging, R134a forms droplets on the surface of the aqueous solution, indicating oversaturation of tetrafluoroethane in the gas phase under the experimental temperature and pressure conditions. Visual observation through the viewing window revealed the rapid formation of the hydrate film at the gas−liquid interface upon initiating cooling at 26 min. Subsequently, a small amount of hydrate started forming along the reactor wall. It was confirmed in Nesterov[21] that the hydrate film is primarily composed of mixed R134a + CO_2 hydrates. The hydrate film exhibited a noticeable barrier effect on CO_2. Throughout the experiment, no significant generation of CO_2 hydrates was

https://doi.org/10.1021/acsomega.3c09839
ACS Omega 2024, 9, 30234−30243

observed. This is attributed to the hindrance caused by the hydrate film, impeding subsequent gas−liquid contact, heat, and mass transfer processes. Consequently, the contact between R134a and CO_2 gas molecules and water molecules was impeded, inhibiting further hydrate growth. As a thermodynamic promoter, the mixed hydrate generated by R134a and CO_2 features a lower phase equilibrium pressure in comparison to that of pure CO_2 hydrate. The formation of mixed R134a + CO_2 hydrates is initiated first, subsequently promoting the generation of CO_2 hydrates. It is comparable to the process in which R134a promotes the formation of pure CO_2 hydrate in our prior work.[20] As a result, only a small amount of hydrates generated along the reactor wall and the gas−liquid interface by the end of the 300 min experiment.

The experiments results proved that the addition of SDS caused significant changes in the growth process of hydrates. The control experiment was conducted at an initial charge temperature of 12 °C. In the presence of 500 ppm of SDS in deionized water (as depicted in Figure 3b), after being pressurized, R134a floats on the gas−liquid interface in the form of liquid droplets due to its effect of surface tension. Via its promoting effect, a mixed hydrate film of R134a and CO_2 is formed. At the 5 min mark, a substantial growth of hydrates along the reactor wall is observed through the visual window, indicating an upward progression. Notably, at the gas−liquid interface, no hydrate film formation is observed during the growth process, signifying that the added SDS effectively disrupts or prevents the generation of hydrate films at the gas−liquid interface during the hydrate growth process. Under the capillary action of SDS surfactants, liquid water is transported upward along the reactor wall.[21,28,29] This phenomenon aligns with prior research demonstrating similar effects of SDS in promoting R134a/CO_2 interactions. As the hydrates grow upward along the reactor wall, a portion of the hydrates formed in close proximity to the wall descends into the aqueous solution due to their own gravitational force. This phenomenon is attributed to the less dense structure of hydrates formed under the influence of SDS. At this time, the heat transfer rate of the reactor wall is accelerated, and a large amount of new hydrate starts to be generated until the hydrate growth is completely finished and the temperature stabilizes. The quantity of hydrates generated is significantly greater than that depicted in Figure 3a. When using R134a as the sole promoting agent, a noticeable hydrate film forms at the gas−liquid interface, impeding gas−liquid contact. The addition of SDS disrupts the formation of the hydrate film, creating gas−liquid channels within the already formed hydrates, thus promoting the extensive generation of hydrates. On the basis of the previous growth model combined with the experimental phenomenon, the growth model of R134a and CO_2 mixed hydrate is established as in Figure 3c.

From Figure 4, it is evident that the temperature−pressure curves in the 500 ppm of SDS aqueous solution exhibit rapid temperature rise and pressure decline at corresponding times, aligning with the rapid generation of hydrates observed through the visual window. This validates the significant synergistic effect of SDS in promoting the CO_2/H_2 hydrate-based separation with R134a. Under the 0 ppm of SDS condition, there is a slight initial pressure decrease followed by stabilization, consistent with the phenomenon where hydrate film formation hinders further hydrate generation. Conversely, under the 500 ppm of SDS condition, there is a further decrease in pressure, indicating enhanced hydrate formation upon SDS addition. This reaffirms the disruptive effect of SDS on the hydrate film. The separation

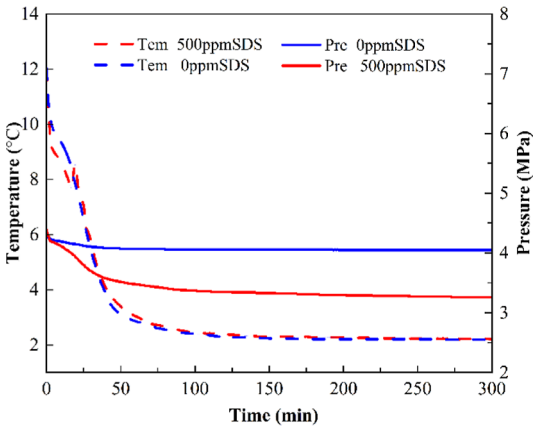

Figure 4. Changes of temperature and pressure curves using 3.5_{mol} % R134a coupled with 0 and 500 ppm of SDS.

efficiencies and separation coefficients derived from the two experimental groups were then calculated separately, and the H_2 separation effect was compared with the adsorption of pure water. At the end of the experiment, it was calculated by gas chromatography measurements that the gas-phase H_2 concentration increased from 46.87 to 54.88% and the CO_2 separation efficiency increased from 5.26 to 36.93% after the addition of 500 ppm of SDS.

3.2. Effect of Different SDS Concentration Synergistic R134a on the Separation Process of CO_2/H_2 Hydrate Method. *3.2.1. Changes of Hydrate Growth Process during the Separation Process of Hydrate Method.* The addition of SDS concentration has a significant impact on the hydrate generation process. Under an initial charge temperature of 12 °C, experiments on CO_2/H_2/R134a hydrate formation were conducted with different concentrations of SDS aqueous solution (0−1000 ppm), and the $P-T$ curves of the hydrate formation process are shown in Figure 5.

In the 0 ppm of SDS aqueous solution, the temperature curve of the R134a/CO_2/H_2 separation experiment gradually decreased from 12 °C to the set temperature, and no significant temperature rise was observed throughout the process. When R134a/CO_2/H_2 is separated in pure water, the pressure decreases first, and the pressure no longer decreases after the hydrate film is generated at the gas−liquid interface. This pressure change is due to the formation of a hydrate film that blocks subsequent gas−liquid contact and heat and mass transfer processes. In the 100 ppm of SDS aqueous solution, a small temperature rise appeared at 6 min, followed by a continued temperature decrease until a significant temperature rise occurred at 32 min. At 6 min, the heat released from the generation of a small amount of hydrate was countered by the cooling capacity provided by the refrigeration unit. As the rate of hydrate formation increased, the heat released surpassed the cooling capacity at 32 min, resulting in a substantial temperature rise. With an increase in SDS concentration, the initial temperature rise followed by cooling gradually disappeared. This is due to the accelerated rate of hydrate formation, which releases heat beyond the cooling capacity of the refrigeration unit. Through the viewing window, it was observed that in high-concentration SDS solutions, hydrates began to generate rapidly along the reactor wall in a short period. After a certain amount of hydrates grew along the reactor wall, the hydrates generated close to the wall hindered the capillary action of SDS, leading to a reduction in the rate of hydrate formation, less heat release, and

https://doi.org/10.1021/acsomega.3c09839
ACS Omega 2024, 9, 30234−30243

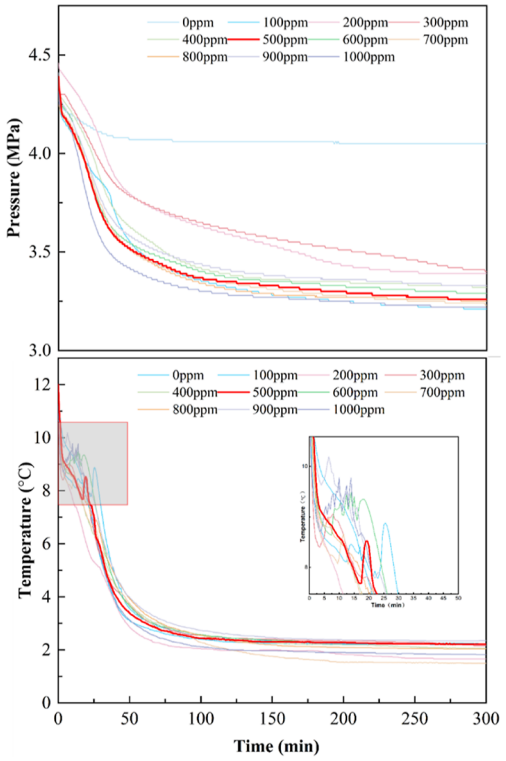

Figure 5. Temperature and pressure curves of hydrate formation with different SDS concentrations.

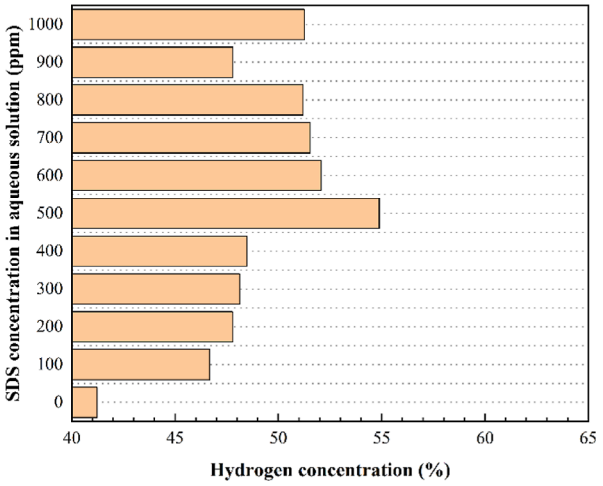

Figure 6. Induction time of SDS aqueous solution with different concentrations.

a decrease in temperature. Subsequently, the hydrates started to slide into the aqueous solution due to their own gravity. It caused by the less dense structure of the hydrates formed under the influence of SDS. At the same time, the heat transfer rate along the reactor wall increased, and new hydrates began to generate rapidly along the wall, causing the temperature to rise again until the complete end of hydrate growth and temperature stabilization.

The induction time also changed with the change of SDS concentration. The induction times remain within 7 min, regardless of the variation in SDS concentration. The shortest induction time of 3 min was observed at SDS concentrations of 300 ppm. The gas consumption during the experiment gradually increases with the rise in SDS concentration, reaching its maximum at the end of the 500 ppm experiment. The gas consumption remained relatively constant above 500 ppm for SDS.

3.2.2. Effect of Different SDS Concentration on the Separation Effect of H_2. The variations in hydrate growth directly impact the separation efficiency. Figures 6 and 7 illustrate the influence of different SDS concentrations on the separation efficiency of the mixed gases. In pure water, the CO_2 separation efficiency is 5.26%, the separation factor is 1.31, and the H_2 concentration is 42.31%. At an SDS concentration of 100 ppm, the CO_2 separation efficiency increases to 24.16%, with a separation factor of 15.21, and the H_2 concentration rises to 47.67%. This is an improvement compared to conditions without SDS. In low-concentration SDS aqueous solutions, the promotion of CO_2 hydrate formation in the mixed gas by R134a is not effective. The role of R134a as a thermodynamic promoter in lowering the phase equilibrium conditions for CO_2 hydrate formation. Furthermore, as the SDS concentration increases, CO_2 hydrate formation becomes more pronounced. The H_2 concentration in the residual gas after reaction equilibrium shows a gradual increase followed by a decrease with the increase in SDS aqueous solution concentration. When the SDS solution concentration reaches 500 ppm, the CO_2 separation efficiency, separation factor, and H_2 concentration in the residual gas phase reach their maximum values at 36.03, 25.97, and 54.88%, respectively. The H_2 concentration increases by 16.38% compared to the feed gas, showing performance comparable to traditional chemical additives such as THF and TBAB in a static environment.[18,30] With the increasing concentration of SDS in the aqueous solution, the CO_2 separation efficiency initially rises, reaching a peak around 500 ppm of SDS concentration, and then decreases. Similarly, the separation factor and postseparation H_2 concentration show an initial increase followed by a decrease. In summary, based on the conclusions and analyses, the synergistic growth effect of R134a and CO_2 hydrates is most effective at an SDS concentration of 500 ppm, resulting in the best CO_2 separation efficiency.

3.3. Effect of Initial Charge Temperatures on the Separation Process of Hydrate Method. *3.3.1. Effect of Different Initial Charge Temperatures on Induction Time.* Initial charge temperature is an influencing factor that promotes the synergistic generation of R134a hydrate and CO_2 hydrate. The rapid nucleation of R134a hydrates caused by cooling significantly influences the growth rate of CO_2 hydrates. To further explore the generation process of hydrates at different initial charge temperatures, we investigated the formation process of 3.5_{mol} % R134a/CO_2/H_2 hydrates with 500 ppm of SDS at various charging temperatures.

The temperature−pressure diagrams for hydrate growth at different charging temperatures are shown in Figure 8, with panel (a) illustrating the pressure curves and panel (b) displaying the temperature curves. The time interval between the completion of initial loading and the initiation of hydrate nucleation is defined as the induction time, consistent with the definition of the induction time in Takeya.[31] Combined with the observations from high-definition cameras and analysis of temperature change curves (which were used to determine the start time of hydrate nucleation), the induction times under different loading temperatures are illustrated in Figure 9. As the initial charge temperature decreases, the induction time required for hydrate formation becomes progressively shorter, decreasing from 41 min at an initial temperature of 18 °C to 3.6 min at 9 °C.

https://doi.org/10.1021/acsomega.3c09839
ACS Omega 2024, 9, 30234−30243

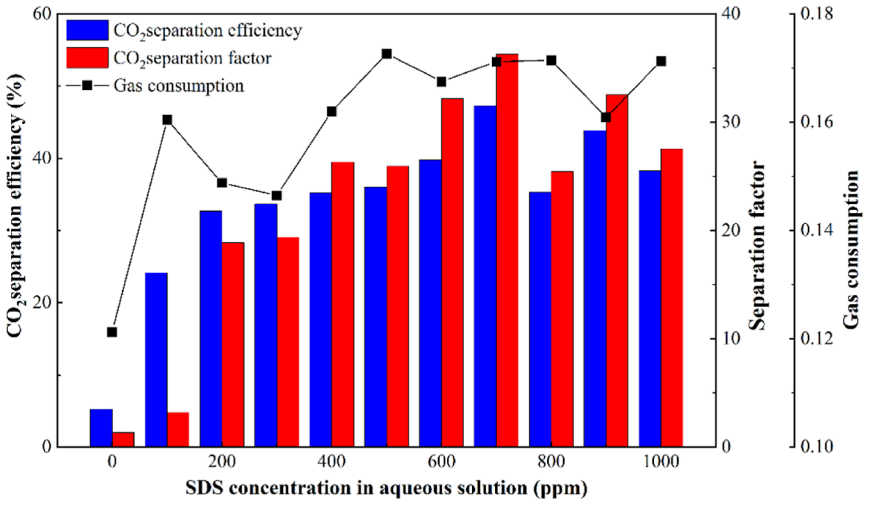

Figure 7. Influence of SDS concentration on CO_2 separation performance.

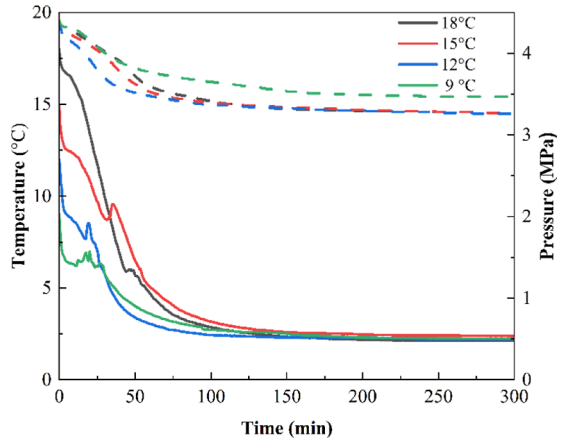

Figure 8. Temperature−pressure curves for hydrate generation at different initial charge temperatures.

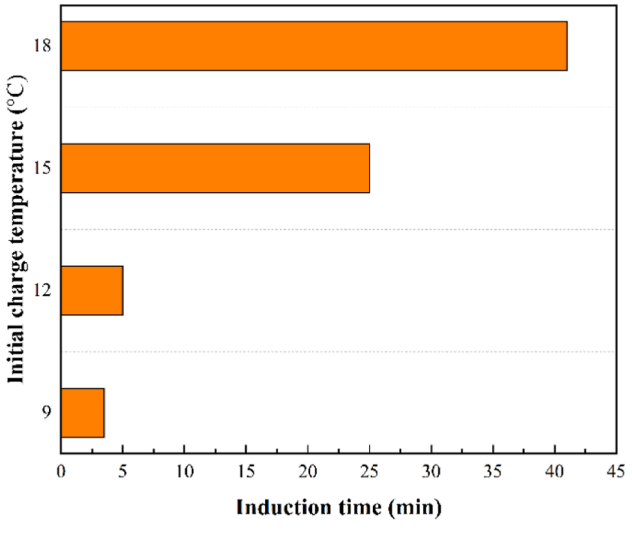

Figure 9. Induction time for hydrate generation at different initial charge temperatures.

Lower charging temperatures expedite the attainment of phase equilibrium conditions necessary for the rapid generation of R134a/CO_2/H_2 hydrates. Analyzing the temperature−pressure curves during hydrate formation reveals that, at higher initial charging temperatures, pure water initially absorbs and separates the mixed gases, resulting in a decrease in pressure without the occurrence of a temperature rise indicative of hydrate formation. As the temperature gradually decreases, the R134a/CO_2/H_2 mixed gas system in the SDS aqueous solution reaches the phase equilibrium conditions for hydrate generation. This leads to a large amount of hydrate production, corresponding to a large temperature peak in the $P-T$ diagram as the initial charge temperature decreases and the pressure profile begins to decrease rapidly, as shown in Figure 8. The experiment reaches equilibrium when the temperature stabilizes, all R134a in the reactor is completely consumed, and the system achieves a balanced state. There was a significant effect on the induction time at the end of each experiment at different initial charge temperatures, but not on the pressure and gas consumption at the equilibrium of the reaction. It was noted that the gas consumption reached a maximum of 0.1727 mol of gas at 12 °C, indicating that the synergistic effect of R134a and CO_2 hydrate generation is most effective at this temperature.

3.3.2. Effect of Initial Charge Temperatures on Gas Consumption Rate and Separation Efficiency. The influence of initial charge temperature on gas consumption rate is significant. Gas consumption rate is expressed through pressure drop eq 5, where a smaller tend indicates a faster reaction rate when the pressure drop ΔP is relatively close. When both ΔP and t_{end} values are small, it indicates that the hydrate reaction is coming to an end and the pressure drop rate and hydrate generation are not satisfactory. Based on the effective reaction time t_{end} with and the pressure drop ΔP at the end of the effective reaction time the average pressure drop of the hydration reaction, the average pressure drop rate ΔP_m can be calculated to respond to the rate of gas consumption in the aqueous solution of 500 ppm of SDS at different initial charge temperatures.

Calculation results reveal that as the initial charge temperature decreases, the effective reaction time continuously shortens (Figure 10). At 9 °C, the shortest effective reaction time is 40 min, but the pressure drop ΔP at this point is 0.51 MPa, with an average pressure drop rate of 0.765 MPa/h. This demonstrates that, under these conditions, the synergistic effect of R134a and CO_2 hydrate formation is not significant. Simultaneously, with the decrease in initial charge temperature, the pressure driving force and average pressure drop rate initially increase and then

https://doi.org/10.1021/acsomega.3c09839
ACS Omega 2024, 9, 30234−30243

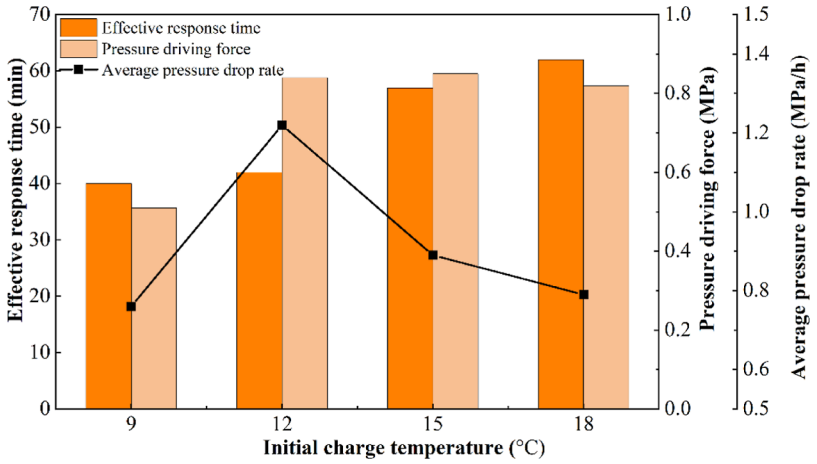

Figure 10. Effective reaction time and pressure drive force at different initial charge temperatures.

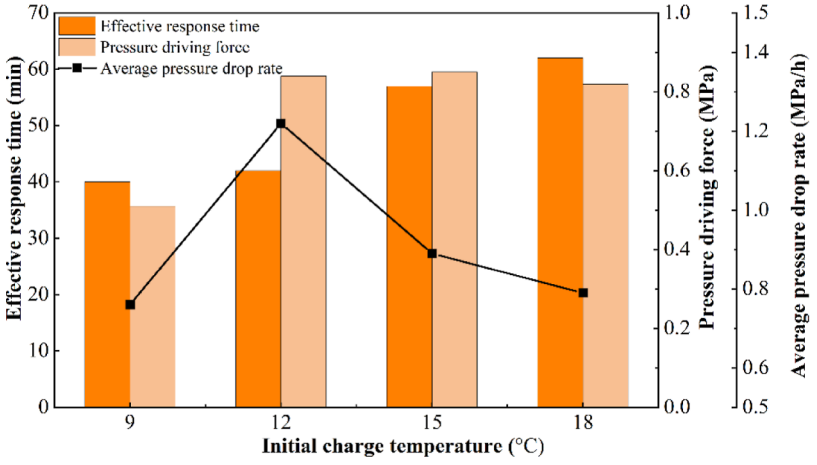

Figure 11. H_2 concentration and separation effects at different initial charge temperatures.

decrease. At an initial charge temperature of 12 °C in a 500 ppm of SDS aqueous solution, the effective reaction time is 42 min, and at the end of the effective reaction, the pressure in the reaction vessel is 3.56 MPa, with a pressure drop of 0.84 MPa. The maximum average pressure drop rate was 1.2 MPa/h, indicating that under these conditions, R134a synergistically promotes the most significant rate of CO_2 consumption in the gas mixture.

In the process of gas separation from hydrates, as the initial charge temperature decreases, the separation efficiency initially increases and then decreases (Figure 11). At 12 °C, the separation efficiency of hydrates is most prominent, demonstrating that at an initial charge initial charge temperature of 12 °C, R134a promotes the generation of more CO_2 hydrates, resulting in better separation efficiency.

4. CONCLUSIONS

In addressing the limitations of the hydrate method in the separation of CO_2/H_2 mixed gases, this study employs thermodynamic promoter R134a in conjunction with kinetic promoter SDS to enhance hydrate growth and optimize the separation of CO_2/H_2 mixed gases. The impact of different SDS concentrations in synergy with 3.5_{mol} % R134a and varying initial charge temperatures on the effectiveness of hydrate-based separation is investigated. The main findings are as follows:

In the absence of SDS, 3.5_{mol} % R134a initially forms a hydrate membrane at the gas−liquid interface, impeding gas−liquid contact and hindering the extensive generation of CO_2 hydrates. The introduction of SDS creates gas−liquid exchange channels within the R134a hydrate membrane, preventing the formation of the membrane and facilitating gas−liquid exchange, leading to a significant increase in the production of CO_2 hydrates in the mixed gas.

With increasing SDS concentration, the amount of CO_2/H_2 mixed gas hydrate generation, gas consumption, separation efficiency, and H_2 concentration exhibit an initial increase followed by a decrease. Optimal separation efficiency and maximum H_2 concentration are achieved at an SDS concentration of 500 ppm.

As the initial charge temperature decreased, the induction time gradually shortened, but there is no significant improvement in hydrate generation rate and effectiveness. Considering overall factors, the optimum initial charge temperature is determined to be 12 °C, the promoter effect of R134a is most significant at this temperature.

At an initial charge temperature of 12 °C in a 500 ppm of SDS aqueous solution, the best hydrate generation and separation efficiency are observed. Under these conditions, the H_2 concentration is 54.88%, with separation efficiency and separation factor reaching 42.29 and 27.34, respectively, and the induction time is reduced to 5 min. The results of this study

https://doi.org/10.1021/acsomega.3c09839
ACS Omega 2024, 9, 30234−30243

provide a better reference for the advancement of hydrate separation technology.

AUTHOR INFORMATION

Corresponding Authors

Yanqiu Xiao − *Zhengzhou University of Light Industry, Zhengzhou 450002, China*; Email: xiaoyanqiu@zzuli.edu.cn

Chuanxiao Cheng − *Zhengzhou University of Light Industry, Zhengzhou 450002, China*; orcid.org/0000-0001-5057-6364; Email: cxcheng@zzuli.edu.cn

Authors

Tian Qi − *School of Energy and Power Engineering, Zhengzhou University of Light Industry, Zhengzhou 450002, China*; orcid.org/0000-0003-1808-0822

Mengfei Liu − *School of Energy and Power Engineering, Zhengzhou University of Light Industry, Zhengzhou 450002, China*

Zihan Lu − *School of Energy and Power Engineering, Zhengzhou University of Light Industry, Zhengzhou 450002, China*

Qianhao Zhang − *School of Energy and Power Engineering, Zhengzhou University of Light Industry, Zhengzhou 450002, China*

Miao Yang − *City University of Hong Kong, Kowloon, Hong Kong 999077, China*

Lanlan Jiang − *Key Laboratory of Ocean Energy Utilization and Energy Conservation of Ministry of Education, Dalian University of Technology, Dalian 116024, China*; orcid.org/0000-0003-3683-6419

Wenfeng Hu − *School of Energy and Power Engineering, Zhengzhou University of Light Industry, Zhengzhou 450002, China*

Runfeng Tian − *School of Energy and Power Engineering, Zhengzhou University of Light Industry, Zhengzhou 450002, China*

Complete contact information is available at: https://pubs.acs.org/10.1021/acsomega.3c09839

Notes

The authors declare no competing financial interest.

ACKNOWLEDGMENTS

This work was financially supported by Scientific and technological innovation talents project of colleges and universities in Henan Province (23HASTIT017), the Science and Technology project in Henan Province (222102320013 and 232102321084), Henan Province colleges and universities young backbone teacher training program (2020GGJS128), supported by the Key Laboratory of Ocean Energy Utilization and Energy Conservation of Ministry of Education (LOEC-202107), and the Doctoral Scientific Research Foundation of Zhengzhou University of Light Industry (2019BSJJ011).

REFERENCES

(1) Adamu, H.; Bello, U.; Yuguda, A. U.; Tafida, U. I.; Jalam, A. M.; Sabo, A.; Qamar, M. Production processes, techno-economic and policy challenges of bioenergy production from fruit and vegetable wastes. *Renewable Sustainable Energy Rev.* **2023**, *186*, 113686.

(2) Demirbas, A. Biofuels sources, biofuel policy, biofuel economy and global biofuel projections. *Energy Convers. Manage.* **2008**, *49* (8), 2106−2116.

(3) Xiang, G.; Zhang, Q.; Li, Y.; Zhang, X.; Liu, H.; Lu, C.; Zhang, H. Enhancement on photobiological hydrogen production from corn stalk via reducing hydrogen pressure in bioreactors by way of phased decompression schemes. *Bioresour. Technol.* **2023**, *385*, 129377.

(4) Łukajtis, R.; Hołowacz, I.; Kucharska, K.; Glinka, M.; Rybarczyk, P.; Przyjazny, A.; Kamiński, M. Hydrogen production from biomass using dark fermentation. *Renewable Sustainable Energy Rev.* **2018**, *91*, 665−694.

(5) Bonalumi, D.; Giuffrida, A. Investigations of an air-blown integrated gasification combined cycle fired with high-sulphur coal with post-combustion carbon capture by aqueous ammonia. *Energy* **2016**, *117*, 439−449.

(6) Mondal, M. K.; Balsora, H. K.; Varshney, P. Progress and trends in CO_2 capture/separation technologies: A review. *Energy* **2012**, *46* (1), 431−441.

(7) Ahmed, R.; Liu, G.; Yousaf, B.; Abbas, Q.; Ullah, H.; Ali, M. U. Recent advances in carbon-based renewable adsorbent for selective carbon dioxide capture and separation-A review. *J. Clean. Prod.* **2020**, *242*, 118409.

(8) Yan, Z.; Zhang, M.; Shi, F.; Zhu, B.; Liu, M.; Wang, S.; Li, Y.; Nunes, S. P. Enhanced CO_2 separation in membranes with anion-cation dual pathways. *J. CO2 Util.* **2020**, *38*, 355−365.

(9) Lee, Y.; Kim, H.; Lee, W.; Kang, D. W.; Lee, J. W.; Ahn, Y.-H. Thermodynamic and kinetic properties of CO_2 hydrates and their applications in CO_2 capture and separation. *J. Environ. Chem. Eng.* **2023**, *11* (5), 110933.

(10) Sun, Q.; Kang, Y. T. Review on CO_2 hydrate formation/dissociation and its cold energy application. *Renewable Sustainable Energy Rev.* **2016**, *62*, 478−494.

(11) Bundhoo, Z. M. A. Potential of bio-hydrogen production from dark fermentation of crop residues: A review. *Int. J. Hydrogen Energy* **2019**, *44* (32), 17346−17362.

(12) Xia, Z.; Zhao, Q.; Chen, Z.; Li, X.; Zhang, Y.; Xu, C.; Yan, K. Review of methods and applications for promoting gas hydrate formation process. *J. Nat. Gas Sci. Eng.* **2022**, *101*, 104528.

(13) Wu, W.; Hao, B.; Guo, Y.; Yang, J.; Du, M.; Zheng, Q.; Bai, Z. Application of monocyclic compounds as natural gas hydrate promoters: A review. *Chem. Eng. Res. Des.* **2023**, *190*, 66−90.

(14) Chen, Z.; Fang, J.; Xu, C.; Xia, Z.; Yan, K.; Li, X. Carbon dioxide hydrate separation from Integrated Gasification Combined Cycle (IGCC) syngas by a novel hydrate heat-mass coupling method. *Energy* **2020**, *199*, 117420.

(15) Duc, N. H.; Chauvy, F.; Herri, J.-M. CO_2 capture by hydrate crystallization - A potential solution for gas emission of steelmaking industry. *Energy Convers. Manage.* **2007**, *48* (4), 1313−1322.

(16) Cheng, C.; Wang, F.; Tian, Y.; Wu, X.; Zheng, J.; Zhang, J.; Li, L.; Yang, P.; Zhao, J. Review and prospects of hydrate cold storage technology. *Renewable Sustainable Energy Rev.* **2020**, *117*, 109492.

(17) Babu, P.; Kumar, R.; Linga, P. Medium pressure hydrate based gas separation (HBGS) process for pre-combustion capture of carbon dioxide employing a novel fixed bed reactor. *Int. J. Greenh. Gas Control* **2013**, *17*, 206−214.

(18) Cheng, C.; Zhang, J.; Song, T.; Xiao, Y.; Jin, T.; Wu, X.; Liu, J.; Zhu, S.; Qi, T.; Hu, W.; Zhang, J.; Ma, J.; Han, Y.; Wang, J.; Zhao, J.; Zhang, L. Rapid and uniform nucleation, growth, and high-density cold storage of tetra-n-butylammonium bromide hydrate in a pilot-scale space. *J. Energy Storage* **2024**, *86*, 111127.

(19) Lee, H.; Park, C.; Lee, E.; Lee, J. D.; Kim, Y. Effect of HFC-134a as a Promoter of CO_2 Hydrate: Phase Equilibrium, Dissociation Enthalpy and Kinetics. *J. Chem. Eng. Data* **2017**, *62* (12), 4395−4400.

(20) Song, T.; Zhang, J.; Li, W.; Ma, J.; Hu, S.; Liu, J.; Li, X.; Hu, W.; Lan, C.; Tian, G.; et al. Rapid Growth of the CO_2 Hydrate Induced by Mixing Trace Tetrafluoroethane. *ACS Omega* **2023**, *8* (44), 41232−41242.

(21) Nesterov, A. N.; Reshetnikov, A. M. New combination of thermodynamic and kinetic promoters to enhance carbon dioxide hydrate formation under static conditions. *Chem. Eng. J.* **2019**, *378*, 122165.

(22) Lirio, C. F. d. S.; Pessoa, F. L. P.; Uller, A. M. C. Storage capacity of carbon dioxide hydrates in the presence of sodium dodecyl sulfate (SDS) and tetrahydrofuran (THF). *Chem. Eng. Sci.* **2013**, *96*, 118−123.

https://doi.org/10.1021/acsomega.3c09839
ACS Omega 2024, 9, 30234−30243

(23) Linga, P.; Kumar, R.; Lee, J. D.; Ripmeester, J.; Englezos, P. A new apparatus to enhance the rate of gas hydrate formation: Application to capture of carbon dioxide. *Int. J. Greenh. Gas Control* **2010**, *4* (4), 630−637.
(24) Kang, S. P.; Lee, J.; Seo, Y. Pre-combustion capture of CO_2 by gas hydrate formation in silica gel pore structure. *Chem. Eng. J.* **2013**, *218*, 126−132.
(25) Linga, P.; Kumar, R.; Englezos, P. The clathrate hydrate process for post and pre-combustion capture of carbon dioxide. *J. Hazard. Mater.* **2007**, *149* (3), 625−629.
(26) Smith, J. M. Introduction to chemical engineering thermodynamics. *J. Chem. Educ.* **1950**, *27* (10), 584.
(27) Linga, P.; Kumar, R.; Englezos, P. Gas hydrate formation from hydrogen/carbon dioxide and nitrogen/carbon dioxide gas mixtures. *Chem. Eng. Sci.* **2007**, *62* (16), 4268−4276.
(28) Lo, C.; Zhang, J.; Somasundaran, P.; Lee, J. W. Investigations of surfactant effects on gas hydrate formation via infrared spectroscopy. *J. Colloid Interface Sci.* **2012**, *376* (1), 173−176.
(29) Gayet, P.; Dicharry, C.; Marion, G.; Graciaa, A.; Lachaise, J.; Nesterov, A. Experimental determination of methane hydrate dissociation curve up to 55 MPa by using a small amount of surfactant as hydrate promoter. *Chem. Eng. Sci.* **2005**, *60* (21), 5751−5758.
(30) Zhong, D. L.; Wang, Y. R.; Lu, Y. Y.; Wang, W. C.; Wang, J. L. Phase equilibrium and kinetics of gas hydrates formed from CO_2/H_2 in the presence of tetrahydrofuran and cyclohexane. *J. Nat. Gas Sci. Eng.* **2016**, *35*, 1566−1572.
(31) Takeya, S.; Hori, A.; Hondoh, T.; Uchida, T. Freezing-Memory Effect of Water on Nucleation of CO_2 Hydrate Crystals. *J. Phys. Chem. B* **2000**, *104* (17), 4164−4168.

https://doi.org/10.1021/acsomega.3c09839
ACS Omega 2024, 9, 30234−30243